

On algebraic bounds for POSM and MRAS

Martin J. Gander and Michal Outrata

Abstract We show for a model problem that the MRAS bound is not the natural analogue of the POSM bound, i.e., there is seemingly a gap between the continuous and discrete representations of the same bound (see, e.g., [2, 1]). We then reformulate the original MRAS bound so that we get a piece by piece correspondence of the discrete and continuous factors. This allows for a direct use of the known results obtained at the continuous level in the discrete method, without the need for re-calculation of the optimized parameters specifically for MRAS. This becomes especially useful in more involved settings where the recalculation of the optimized parameters specifically for the discrete setting can be non-trivial.

1 Introduction and preliminaries

We consider the Poisson equation as our model problem, i.e.,

$$\Delta u = f \quad \text{in } \Omega := (-a, a) \times (0, b) \quad \text{and} \quad u = g \quad \text{on } \partial\Omega, \quad (1)$$

where f and g are given. We decompose Ω into two subdomains $\Omega_1 := (-a, L/2) \times (0, b)$ and $\Omega_2 := (-L/2, a) \times (0, b)$ with interfaces Γ_1 and Γ_2 , overlap $O := (-L/2, L/2) \times (0, b)$ (if $L > 0$) and complements $\Theta_2 := \Omega \setminus \Omega_1$ and $\Theta_1 := \Omega \setminus \Omega_2$. Creating an equidistant mesh on Ω with mesh size h , we denote by $N_r + 1$ the number of grid rows and $N_c + 1$ the number of grid columns, see Figure 1 (left). We also define the one-grid-column-prolonged subdomains $\Omega_1^h := (-a, L/2 + h) \times (0, b)$ and $\Omega_2^h := (-L/2 - h, a) \times (0, b)$ and also their interfaces $\Gamma_1^h := (L/2 + h) \times (0, b)$ and $\Gamma_2^h := (-L/2 - h) \times (0, b)$. We discretize (1) (right) with a finite difference scheme,

Martin J. Gander
University of Geneva, e-mail: martin.gander@unige.ch

Michal Outrata
University of Geneva, e-mail: michal.outrata@unige.ch

where we introduced the discrete transmission conditions in the last block row of $[A_{\Omega_1} \ A_{\Omega_1, \Omega_2}]$ and the first block row of $[A_{\Omega_2, \Omega_1} \ A_{\Omega_2}]$, which are now given by

$$\tilde{A}_{\Gamma_1} := A_{\Gamma_1} + D, \quad \tilde{A}_{\Gamma_1, \Gamma_1} := -D \quad \text{and} \quad \tilde{A}_{\Gamma_2} := A_{\Gamma_2} + D, \quad \tilde{A}_{\Gamma_2, \Gamma_2} := -D.$$

We are interested in the subdomain version of the *modified restricted additive Schwarz* (MRAS¹, see [2]), defined by its iteration matrix T ,

$$T = I - \sum_{i=1}^2 R_{\Omega_i}^T \tilde{A}_{\Omega_i}^{-1} R_{\Omega_i} \tilde{A}_{\text{aug}} \quad \text{with} \quad R_{\Omega_1} = [I_{\Omega_1} \ 0_{\Omega_2}], \quad R_{\Omega_2} = [0_{\Omega_1} \ I_{\Omega_2}]. \quad (5)$$

Notice that the interface block structure of MRAS does *not* match the one in [3, Algorithm 2] but the transmission matrix D is chosen to get fast convergence, analogously to the parameter p in POSM. Setting

$$\begin{aligned} E_{\Gamma_2}^{\Omega_1} &:= [0_{\Theta_1} I_{\Gamma_2} 0_O 0_{\Gamma_1}]^T, \quad E_{\Gamma_1}^{\Omega_1} := [0_{\Theta_1} 0_{\Gamma_2} 0_O I_{\Gamma_1}]^T, \quad E_{\Theta_1}^{\Omega_1} := [A_{\Gamma_2, \Theta_1} 0_{\Gamma_2} 0_O 0_{\Gamma_1}]^T, \\ E_{\Gamma_2}^{\Omega_2} &:= [I_{\Gamma_2} 0_O 0_{\Gamma_1} 0_{\Theta_2}]^T, \quad E_{\Gamma_1}^{\Omega_2} := [0_{\Gamma_2} 0_O I_{\Gamma_1} 0_{\Theta_2}]^T, \quad E_{\Theta_2}^{\Omega_2} := [0_{\Gamma_2} 0_O 0_{\Gamma_1} A_{\Theta_2, \Gamma_1}]^T, \end{aligned}$$

we can write

$$\tilde{A}_{\Omega_i} = A_{\Omega_i} + E_{\Gamma_i}^{\Omega_i} D \left(E_{\Gamma_i}^{\Omega_i} \right)^T, \quad i = 1, 2,$$

and formulate a convergence result for MRAS, analogue to [2, Theorem 3.2].

Theorem 1 ([2, Section 3])

The MRAS iteration matrix T in (5) has the structure

$$T = \begin{bmatrix} 0 & K \\ L & 0 \end{bmatrix}, \quad \begin{aligned} K &:= A_{\Omega_1}^{-1} E_{\Gamma_1}^{\Omega_1} \left[I + D(A_{\Omega_1}^{-1})_{\Gamma_1, \Gamma_1} \right]^{-1} \left(-D(E_{\Gamma_1}^{\Omega_2})^T + (E_{\Theta_2}^{\Omega_2})^T \right), \\ L &:= A_{\Omega_2}^{-1} E_{\Gamma_2}^{\Omega_2} \left[I + D(A_{\Omega_2}^{-1})_{\Gamma_2, \Gamma_2} \right]^{-1} \left(-D(E_{\Gamma_2}^{\Omega_1})^T + (E_{\Theta_1}^{\Omega_1})^T \right). \end{aligned} \quad (6)$$

Moreover, the asymptotic convergence factor of MRAS is bounded by

$$\begin{aligned} &\sqrt{\|M_1 B_1\|_2 \cdot \|M_2 B_2\|_2}, \\ M_1 &:= \left[I + D(A_{\Omega_1}^{-1})_{\Gamma_1, \Gamma_1} \right]^{-1} \left(-D - A_{\Gamma_1, \Theta_2} A_{\Theta_2}^{-1} A_{\Theta_2, \Gamma_1} \right), \quad B_1 := (A_{\Omega_2}^{-1})_{\Gamma_1, \Gamma_2}, \\ M_2 &:= \left[I + D(A_{\Omega_2}^{-1})_{\Gamma_2, \Gamma_2} \right]^{-1} \left(-D - A_{\Gamma_2, \Theta_1} A_{\Theta_1}^{-1} A_{\Theta_1, \Gamma_2} \right), \quad B_2 := (A_{\Omega_1}^{-1})_{\Gamma_2, \Gamma_1}. \end{aligned} \quad (7)$$

Due to the symmetry of the model problem and the method we have $\tilde{B} := B_1 = B_2$ and $\tilde{M} := M_1 = M_2$, which in turn simplifies the bound in (7) to $\|\tilde{M}\tilde{B}\|_2$.

¹ MRAS was introduced in the so-called *globally deferred correction form*, where we iterate on the global solution unknowns, in contrast to iterating on the subdomain solution unknowns here. This is but a technicality and hence we keep the name; the equivalence is shown in [3, Section 6.1, 6.2].

2 Analysis of the MRAS bound and its reformulation

First, we recall the sine series expansion in the y direction \mathcal{F}_y , so that we have

$$u(x, y) = \sum_{k=1}^{+\infty} \mathcal{F}_y u(x, k) \sin\left(\frac{k\pi}{b}y\right) \equiv \sum_{k=1}^{+\infty} \hat{u}(x, k) \sin\left(\frac{k\pi}{b}y\right),$$

with ${}^2 \mathcal{F}_y u := \int_0^b u(x, y) \sin(k\pi y/b) dy$. Next, we factor out $(A_{\Omega_1}^{-1})_{\Gamma_1, \Gamma_1}$ and $(A_{\Omega_2}^{-1})_{\Gamma_2, \Gamma_2}$ on the left from $M_{1,2}$, so that instead of (7) we focus on the asymptotically equivalent

$$MB := \underbrace{\left[\left((A_{\Omega_1}^{-1})_{\Gamma_1, \Gamma_1} \right)^{-1} + D \right]^{-1}}_{(T \text{ Denom})^{-1}} \underbrace{\left(-D - A_{\Gamma_1, \Theta_2} A_{\Theta_2}^{-1} A_{\Theta_2, \Gamma_1} \right)}_{T \text{ Numer}} \underbrace{\left((A_{\Omega_2}^{-1})_{\Gamma_1, \Gamma_2} \left((A_{\Omega_2}^{-1})_{\Gamma_2, \Gamma_2} \right)^{-1} \right)}_{T \text{ Over}}. \quad (8)$$

The key question is whether the bound (7), which now becomes $\|MB\|$, is the discrete analogue of (3) – piece by piece. Linking each of the blocks in (8) to a discrete linear operator with a continuous counterpart, we analyze it using the Fourier series expansion. Taking $\mathbf{b} \in \mathbb{R}^{N_r-1}$ and interpolating it to a function $\gamma : \Gamma_1^h \rightarrow \mathbb{R}$, the following problems are equivalent up to the FD discretization:

$$A_{\Omega_1} \mathbf{u} = -\frac{1}{h^2} E_{\Gamma_1}^{\Omega_1} \mathbf{b} \quad \text{and} \quad \begin{aligned} \Delta u &= 0 && \text{in } \Omega_1^h, \\ u &= 0 && \text{on } \partial\Omega_1^h \setminus \Gamma_1^h, \quad \text{and} \quad u = \gamma && \text{on } \Gamma_1^h. \end{aligned} \quad (9)$$

Defining the solution operator by $\mathcal{S}_1(\gamma) = u|_{\Gamma_1}$ where u is the solution of (9), we have (up to the FD discretization) the equivalence of the linear operators $-1/h^2 (A_{\Omega_1}^{-1})_{\Gamma_1, \Gamma_1}$ and \mathcal{S}_1 . To calculate \mathcal{S}_1 we expand in the y variable using \mathcal{F}_y , simplifying the continuous problem in (9) to the semi-discrete problem

$$\begin{aligned} \left(\partial_{xx} - \left(\frac{k\pi}{b} \right)^2 \right) \hat{u}(x, k) &= 0 \quad \text{for } x \in (-a, L/2 + h) \text{ and } k \in \mathbb{N}, \\ \hat{u}(-a, k) &= 0 \quad \text{and} \quad \hat{u}(L/2 + h, k) = \hat{\gamma}(k) \quad \text{for } k \in \mathbb{N}, \end{aligned} \quad (10)$$

and denote by $\hat{\mathcal{S}}_1 := \mathcal{F}_y \mathcal{S}_1$ the Fourier symbol of \mathcal{S}_1 . A direct calculation yields

$$\hat{u}(x, k) = \frac{\sinh\left(\frac{k\pi}{b}(a+x)\right) \hat{\gamma}(k)}{\sinh\left(\frac{k\pi}{b}(a+L/2+h)\right)}, \quad \hat{\mathcal{S}}_1 \hat{\gamma}(k) = \frac{\sinh\left(\frac{k\pi}{b}(a+L/2)\right)}{\sinh\left(\frac{k\pi}{b}(a+L/2+h)\right)} \hat{\gamma}(k).$$

Therefore, the eigenvalues of the linear operator $-1/h^2 (A_{\Omega_1}^{-1})_{\Gamma_1, \Gamma_1}$ approximate the modes $k = 1, \dots, N_r - 1$ of $\hat{\mathcal{S}}_1$ given above, as we see in Figure 2. The rest of the

² Using the sine series relies on the Dirichlet boundary conditions (BCs) along $\{y = 0\}$ and $\{y = b\}$ in (1); for different BCs see [4].

block	discrete LO	continuous LO	Fourier symbol
$(A_{\Omega_1}^{-1})_{\Gamma_1, \Gamma_1}$	$-\frac{1}{h^2} (A_{\Omega_1}^{-1})_{\Gamma_1, \Gamma_1}$	$\mathcal{S}_1 : \gamma \mapsto u _{\Gamma_1}$	$\hat{\mathcal{S}}_1 = \frac{\sinh(\frac{k\pi}{b}(a+L/2))}{\sinh(\frac{k\pi}{b}(a+L/2+h))}$
$A_{\Gamma_1, \Theta_2} A_{\Theta_2}^{-1} A_{\Theta_2, \Gamma_1}$	$-h^2 A_{\Gamma_1, \Theta_2} A_{\Theta_2}^{-1} A_{\Theta_2, \Gamma_1}$	$\mathcal{S}_2 : \gamma \mapsto u _{\Gamma_1}$	$\hat{\mathcal{S}}_2 = \frac{\sinh(\frac{k\pi}{b}(a-L/2-h))}{\sinh(\frac{k\pi}{b}(a-L/2))}$
$(A_{\Omega_2}^{-1})_{\Gamma_1, \Gamma_2}$	$-\frac{1}{h^2} (A_{\Omega_2}^{-1})_{\Gamma_1, \Gamma_2}$	$\mathcal{S}_3 : \gamma \mapsto u _{\Gamma_1}$	$\hat{\mathcal{S}}_3 = \frac{\sinh(\frac{k\pi}{b}(a-L/2))}{\sinh(\frac{k\pi}{b}(a+L/2+h))}$
$(A_{\Omega_2}^{-1})_{\Gamma_2, \Gamma_2}$	$-\frac{1}{h^2} (A_{\Omega_2}^{-1})_{\Gamma_2, \Gamma_2}$	$\mathcal{S}_4 : \gamma \mapsto u _{\Gamma_2}$	$\hat{\mathcal{S}}_4 = \frac{\sinh(\frac{k\pi}{b}(a+L/2))}{\sinh(\frac{k\pi}{b}(a+L/2+h))}$

Table 1 The blocks and corresponding linear operators (LO) from (8).

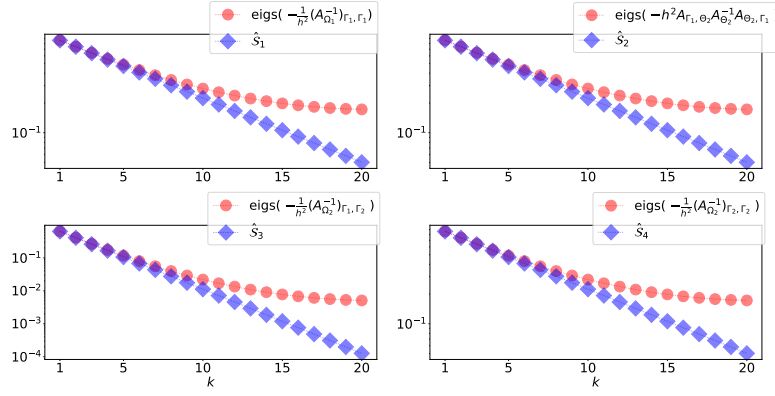


Fig. 2 Results obtained for the parameters $a = b = 1$, $L = 2h$, $N_r = 22$.

blocks in (8) are summarized in Table 1 and illustrated in Figure 2, see [4] for detailed calculations. We see that the approximation is very accurate for the low-frequency modes but not quite accurate for the high-frequency ones. If D diagonalizes in the same basis as the rest of the blocks and we denote its eigenvalues by $\delta_1, \dots, \delta_{N_r-1}$, then the eigenvalues of T^{Denom} , T^{Numer} , T^{Over} approximate certain discrete (truncated) Fourier symbols we present in Table 2 and illustrate in Figure 3. We see that the inaccuracy on the high frequencies is still present. More importantly, comparing Table 2 with (3) shows that the contraction factor due to the domain overlap in (3) matches exactly θ_k for each k , i.e., the one due to the continuous representation of T^{Over} . However, this is clearly *not* the case for the contraction factor due to the transmission condition induced by D . The ratio η_k/ζ_k shows that choosing $\delta_k = p$ (the naive choice) is *not* the correct one (see [4] for more details) and we continue by reformulating Theorem 1 to reflect also the transmission part of (3).

The main tool used to obtain Theorem 1 is the Sherman-Morrison-Woodbury formula for the inverse of a low-rank updated matrix, here the update was the corner block D . We now show that using the same formula for a slightly different block gives the ‘‘correct’’ result. We split the interface blocks as in [3, Section 5.2] and write $A_{\Gamma_1} = A_{\Gamma_1}^L + A_{\Gamma_1}^R$ and $A_{\Gamma_2} = A_{\Gamma_2}^L + A_{\Gamma_2}^R$ so that we have

Theorem 2 *The MRAS iteration matrix T in (5) can also be written as*

$$\bar{T} = \begin{bmatrix} 0 & \bar{K} \\ \bar{L} & 0 \end{bmatrix}, \quad \text{with}$$

$$\begin{aligned} \bar{K} &:= (A_{\Omega_1}^L)^{-1} E_{\Gamma_1}^{\Omega_1} \left((A_{\Omega_1}^L)^{-1} \right)_{\Gamma_1, \Gamma_1}^{-1} \left[\left((A_{\Omega_1}^L)^{-1} \right)_{\Gamma_1, \Gamma_1}^{-1} + \bar{A}_{\Gamma_1} \right]^{-1} \left(-D(E_{\Gamma_1}^{\Omega_2})^T + (E_{\Theta_2}^{\Omega_2})^T \right), \\ \bar{L} &:= (A_{\Omega_2}^R)^{-1} E_{\Gamma_2}^{\Omega_2} \left((A_{\Omega_2}^R)^{-1} \right)_{\Gamma_2, \Gamma_2}^{-1} \left[\left((A_{\Omega_2}^R)^{-1} \right)_{\Gamma_2, \Gamma_2}^{-1} + \bar{A}_{\Gamma_2} \right]^{-1} \left(-D(E_{\Gamma_2}^{\Omega_1})^T + (E_{\Theta_1}^{\Omega_1})^T \right). \end{aligned}$$

Moreover, the asymptotic convergence factor of POSM is bounded by

$$\|\overline{MB}\|_2, \quad \text{where} \quad (12)$$

$$\begin{aligned} \bar{M} &:= (\bar{T}^{Denom})^{-1} \bar{T}^{Numer} = \left[\left((A_{\Omega_1}^L)^{-1} \right)_{\Gamma_1, \Gamma_1}^{-1} + \bar{A}_{\Gamma_1} \right]^{-1} \left((A_{\Gamma_1}^R - A_{\Gamma_1, \Theta_2} A_{\Theta_2}^{-1} A_{\Theta_2, \Gamma_1}) - \bar{A}_{\Gamma_1} \right), \\ \bar{B} &:= \bar{T}^{Over} = (A_{\Omega_2}^R)^{-1} \left((A_{\Omega_2}^R)^{-1} \right)_{\Gamma_2, \Gamma_2}^{-1}. \end{aligned} \quad (13)$$

Focusing on the first block in (13), we take $\mathbf{b} \in \mathbb{R}^{N_r-1}$ and interpolating it to a function $\gamma : \Gamma_1 \rightarrow \mathbb{R}$, the following problems are equivalent up to the FD discretization:

$$A_{\Omega_1}^L \mathbf{u} = -\frac{1}{h} E_{\Gamma_1}^{\Omega_1} \mathbf{b} \quad \text{and} \quad \begin{aligned} \Delta u &= 0 \quad \text{in } \Omega_1, \\ u &= 0 \quad \text{on } \partial\Omega_1 \setminus \Gamma_1, \quad \text{and} \quad \mathbf{n}_1 \cdot \nabla u = \gamma \quad \text{on } \Gamma_1. \end{aligned} \quad (14)$$

Setting $\bar{\mathcal{S}}_2(\gamma) = u|_{\Gamma_1}$, where u is the solution of (14) we have the equivalence (up to the FD discretization) of $-1/h(A_{\Omega_1}^{-1})_{\Gamma_1, \Gamma_1}$ and $\bar{\mathcal{S}}_2$. Considering

$$\begin{aligned} \left(\partial_{xx} - \left(\frac{k\pi}{b} \right)^2 \right) \hat{u}(x, k) &= 0 \quad \text{for } x \in (-a, L/2 + h) \text{ and } k \in \mathbb{N}, \\ \hat{u}(-a, k) &= 0 \quad \text{and} \quad \hat{u}_x(L/2 + h, k) = \hat{\gamma}(k) \quad \text{for } k \in \mathbb{N}, \end{aligned} \quad (15)$$

we set $\hat{\mathcal{S}}_1 := \mathcal{F}_y \bar{\mathcal{S}}_1$ and a direct calculation yields the solution of (15) and $\hat{\mathcal{S}}_1$ as

$$\hat{u}(x, k) = \frac{\sinh\left(\frac{k\pi}{b}(a+x)\right)}{\frac{k\pi}{b} \cosh\left(\frac{k\pi}{b}(a+L/2)\right)}, \quad \hat{\mathcal{S}}_1 \hat{\gamma}(k) = \frac{\sinh\left(\frac{k\pi}{b}(a+L/2)\right)}{\frac{k\pi}{b} \cosh\left(\frac{k\pi}{b}(a+L/2)\right)} \hat{\gamma}(k).$$

Therefore, the eigenvalues of $-1/h((A_{\Omega_1}^L)^{-1})_{\Gamma_1, \Gamma_1}$ approximate the first $N_r - 1$ modes of $\mathcal{F}_y \bar{\mathcal{S}}_1$ with better accuracy in high-frequencies than we observed with \mathcal{S}_1 , see Figure 2 and Figure 4. For the other blocks see Table 3 and Figure 4. If $-\bar{A}_{\Gamma_1}^R$ diagonalizes in the Fourier discrete basis with eigenvalues $\lambda_1, \dots, \lambda_{N_r-1}$, then the eigenvalues of $\bar{T}^{Denom}, \bar{T}^{Numer}, \bar{T}^{Over}$ approximate certain discrete (truncated) Fourier symbols, presented in Table 2 and Figure 3. Notice that at the discrete level we have $MB = \overline{MB}$, i.e., the difference is in the *representation* of the bound (blue markers

block	discrete LO	continuous LO	Fourier symbol
$((A_{\Omega_1}^L)^{-1})_{\Gamma_1, \Gamma_1}$	$-\frac{1}{h} ((A_{\Omega_1}^L)^{-1})_{\Gamma_1, \Gamma_1}$	$\bar{S}_1 : \gamma \mapsto u _{\Gamma_1}$	$\hat{S}_1 = \frac{1}{\frac{k\pi}{b} \coth(\frac{k\pi}{b}(a+L/2))}$
$\bar{A}_{\Gamma_1}^R - A_{\Gamma_1, \Theta_2} A_{\Theta_2}^{-1} A_{\Theta_2, \Gamma_1}$	$-h (\bar{A}_{\Gamma_1}^R - A_{\Gamma_1, \Theta_2} A_{\Theta_2}^{-1} A_{\Theta_2, \Gamma_1})$	$\bar{S}_2 : \gamma \mapsto \mathbf{n}_1 \cdot \nabla u _{\Gamma_1}$	$\hat{S}_2 = \frac{k\pi}{b} \coth(\frac{k\pi}{b}(a-L/2))$
$((A_{\Omega_2}^R)^{-1})_{\Gamma_1, \Gamma_2}$	$-\frac{1}{h} ((A_{\Omega_2}^R)^{-1})_{\Gamma_1, \Gamma_2}$	$\bar{S}_3 : \gamma \mapsto u _{\Gamma_1}$	$\hat{S}_3 = \frac{\sinh(\frac{k\pi}{b}(a-L/2))}{\frac{k\pi}{b} \cosh(\frac{k\pi}{b}(a+L/2))}$
$((A_{\Omega_2}^R)^{-1})_{\Gamma_2, \Gamma_2}$	$-\frac{1}{h} ((A_{\Omega_2}^R)^{-1})_{\Gamma_2, \Gamma_2}$	$\bar{S}_4 : \gamma \mapsto u _{\Gamma_2}$	$\hat{S}_4 = \frac{\sinh(\frac{k\pi}{b}(a+L/2))}{\frac{k\pi}{b} \cosh(\frac{k\pi}{b}(a+L/2))}$

Table 3 The blocks and corresponding linear operators (LO) from (8).

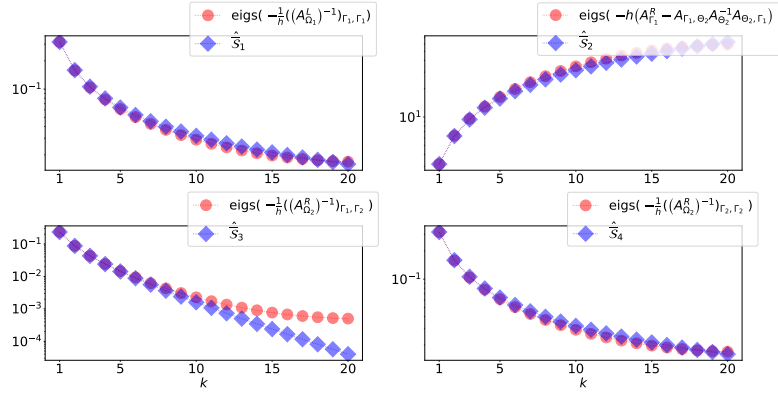


Fig. 4 Results obtained for the parameters $a = b = 1$, $L = 2h$, $N_r = 21$.

in Figure 3) as we changed *only* the block organization in the Sherman-Morrison-Woodbury formula. Comparing Table 2 with (3), we get the link between λ_k (and hence also δ_k) and the Robin parameter p in (3). Calculating the optimal p now directly translates to the optimal choice of D by

$$pI = -hW^T (A_{\Gamma_1}^R + D) W \quad , \text{ i. e., } \quad D = -\frac{p}{h} I - A_{\Gamma_1}^R .$$

References

1. Gander, M.J.: On the influence of geometry on optimized Schwarz methods. *SeMA Journal* **53**(1), 71–78 (2013)
2. Gander, M.J., Loisel, S., Szyld, D.B.: An optimal block iterative method and preconditioner for banded matrices with applications to PDEs on irregular domains. *SIAM Journal on Matrix Analysis and Applications* **33**(2), 653–680 (2012)
3. Gander, M.J., Zhang, H.: A class of iterative solvers for the Helmholtz equation: factorizations, sweeping preconditioners, source transfer, single layer potentials, polarized traces, and optimized Schwarz methods. *SIAM Review* **61**(1), 3–76 (2019)
4. Outrata, M.: Schwarz methods, Schur complements, preconditioning and numerical linear algebra. Ph.D. thesis, University of Geneva, Math Department (2022)